

Profilometry using fringe projection via Fourier Transform (FTP)

Mayra Stefany Gómez Triana* and Juan Pablo Solís Ruiz†
(Dated: December 14, 2025)

In this work we present the application of Fourier Transform Profilometry for the three-dimensional characterization of surfaces in various industrial applications. We discuss the basic principles of the technique, its experimental implementation, and the results obtained in the characterization of different types of surfaces. Our results demonstrate the capability of Fourier Transform Profilometry to provide accurate and detailed measurements of surface topography, making it a valuable tool for industrial and research applications.

I. INTRODUCTION

Humankind has realized the importance of measuring; to measure is to learn, to extend our senses, and thereby obtain more information that helps us make better decisions. Over the last three decades, countless contact and non-contact techniques have been used in science and engineering applications for 3D (three-dimensional) surface reconstruction. However, in recent years, optical sensors for evaluating the 3D shape of an object have played an increasingly important role. The main advantage of optical sensors is that they require no direct contact with the object to be characterized; additionally, these systems are significantly faster than contact-based techniques.

The basic idea is to extract depth-related information from an image efficiently and automatically. Once obtained, this information can be used in various processes such as robotic manipulation, automated inspection, quality control, reverse engineering, 3D navigation maps, and virtual reality. Although several methodologies exist, projection of a fringe pattern is one of the most widely used. Fringe projection methods are used in non-destructive testing, optics, and 3D reconstruction systems. Some characteristics of these systems are high precision, noise immunity, and fast processing.

A commonly used fringe-processing method is Fourier Transform Profilometry (FTP), proposed by Takeda and Mutoh [1] in 1982. Later, Berryman and Pedraza [2] proposed a modification to Fourier profilometry by performing local and global analyses of the wrapped phase; as a result, phase unwrapping algorithms (temporal and spatial) were introduced and modified.

To reconstruct the 3D profile accurately, one of the key issues in Fourier transform profilometry is to extract the first-order spectrum precisely in the spectral domain, which requires an appropriate band-pass filter to retain the maximum first-order spectrum information while keeping it separated from the background spectrum and other higher-order spectra. The conditions to separate these spectral regions have been well studied by considering the minimum distances between them. To

remove the background spectrum, a wavelet transform was applied to separate background illumination terms from a fringe pattern. One method to obtain this spectral region employed a Hanning window defined equally for both horizontal and vertical frequencies.

II. THEORETICAL BACKGROUND

The foundations of profilometry were laid by Takeda [1] in 1983. Takeda's main idea was to project a fringe pattern with a known spatial frequency onto an object and then use the one-dimensional Fourier Transform to analyze the projected fringe pattern. An image of any object with projected fringes can be represented by the following equation:

$$g(x, y) = a(x, y) + b(x, y) \cos[2\pi f_0 x + \phi(x, y)] \quad (1)$$

where $g(x, y)$ is the image intensity at point (x, y) , $a(x, y)$ represents background illumination, $b(x, y)$ is the contrast between light and dark lines, f_0 is the fundamental frequency, and $\phi(x, y)$ is the modulation of the fringe pattern observed by the camera.

The phase $\phi(x, y)$ contains the depth information (Figure ??), while $a(x, y)$ and $b(x, y)$ are undesired variations or noise. In most cases, $\phi(x, y)$, $a(x, y)$, and $b(x, y)$ vary slowly compared to the spatial frequency f_0 . The angle $\phi(x, y)$ is the phase shift caused by the object surface and the projection angle, and it can be expressed as:

$$\phi(x, y) = \phi_0(x, y) + \phi_z(x, y) \quad (2)$$

where $\phi_0(x, y)$ is the phase caused by the projection angle with respect to the reference plane, and $\phi_z(x, y)$ is the phase caused by the object height distribution.

In Figure 2 we have fringes projected by a projector; the fringes reach the object at point H and cross the reference plane at point Dp. Triangles DpHDc and CHF are similar.

$$\frac{h}{d} = \frac{l}{d-h} \quad (3)$$

yielding the following equation:

$$\phi(x, y) = \arctan\left(\frac{h(x, y)}{l}\right) - \frac{\pi}{2} \quad (4)$$

* A01625609; Also at Tec de Monterrey

† A01067387; Also at Tec de Monterrey

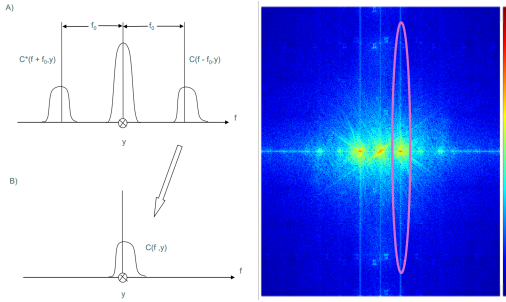


FIG. 1. First-order FT, which contains the phase with depth information.

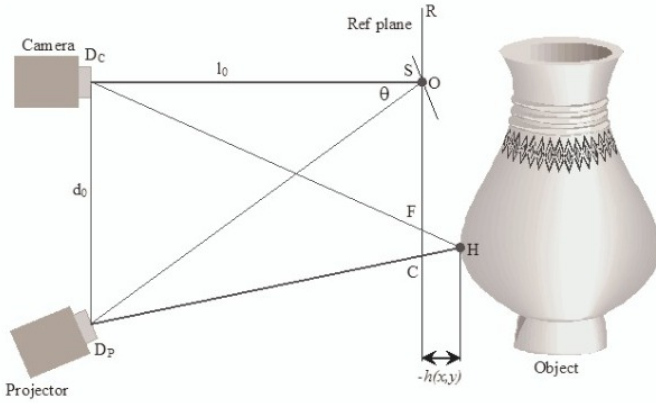


FIG. 2. Experimental configuration.

III. METHODOLOGY

The development of this project was structured into four fundamental phases, ranging from the initial fringe projection to the final processing of the acquired data. Each phase is detailed below.

A. Fringe projection

For the projection, the setup shown in Figure 3 was implemented. Fringe projection was carried out using a Ronchi grating printed on acetate, illuminated by an LED light source. The LED emits a spherical wavefront with an approximate degree of coherence of 0.3[3]. The LED spectrum is shown in Figure 4[4]. The experimental arrangement for fringe projection is described in detail in Figure 2.

Then, once the experimental configuration was correctly assembled, photographs of the objects with projected fringes were captured. The objective was to ensure that the objects contained as many fringes as possible, with high resolution and minimal noise [5]. Images were captured both with the object and without the object; an example is shown in Figure 5.

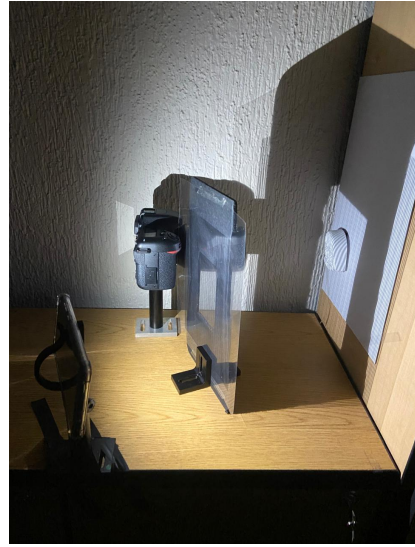


FIG. 3. Experimental configuration.

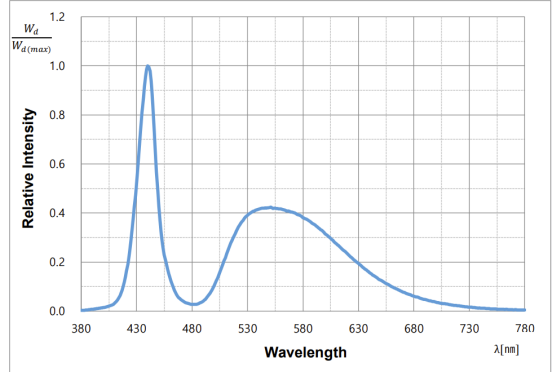


FIG. 4. Emission spectrum of Samsung SPHWH1A1N3A0 white LED.

B. Takeda filtering

As mentioned previously, to obtain an object's topography and extract the image phase, the Fourier transform of the captured image must be computed, and then the



FIG. 5. Example image acquired with fringe projection.

first order must be filtered from the three peaks that appear. Takeda (1983)[1] states that the first order can be filtered using a Hanning window. However, Esquivel (2023)[6] and Chen (2010)[7] recommend using a rectangular or elliptical band-pass filter, as they yield lower error. Nevertheless, for the spectral filtering method used here, a partial Hann window—also known as a Tukey window—was applied to filter the zero-order Fourier component. Subsequently, a square window was applied to the first order, performing the spectral filtering. Two objects were analyzed with this method, and it was developed using a Samsung charger shown in Figure 6 to verify the filtering procedure. Other methodological steps are also shown, but Takeda filtering was the key element for obtaining consistent results. The exact parameters of each window varied, since each image introduced different noise and harmonics in Fourier space.

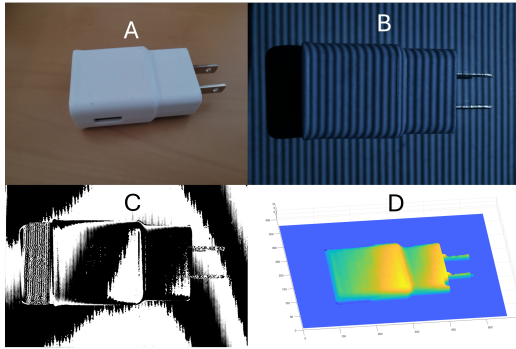


FIG. 6. Images A–D show the prototype used to develop the FTP method.

C. Phase extraction and unwrapping

Phase extraction was performed via the inverse Fourier transform of the already filtered spectrum, as indicated in the FTP process. In this case, the discontinuous phases obtained are within $-\pi$ and π . The phase-unwrapping algorithm by Zixin Zhao (2024)[8] was applied, which uses the transport-of-intensity equation (TIE) in Eq. 5. This equation relates intensity changes with respect to phase, enabling a robust algorithm to correct discontinuities, given an assumed degree of continuity in the intensity flow of the radiation.

$$-k \frac{\partial I(x, y)}{\partial z} = \nabla \cdot [I(x, y) \nabla \cdot \phi(x, y)] \quad (5)$$

D. Phase-to-height conversion and post-processing

For phase-to-height conversion, Figure 7 was used as reference. Based on this, the conversion was performed

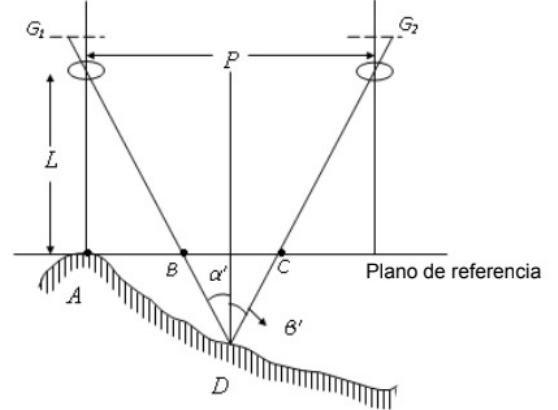


FIG. 7. Experimental configuration.

with the following equation:

$$z(x, y) = \frac{NMbL}{P - NMb} \quad (6)$$

After the initial profilometry, a post-processing step was applied, involving subtraction of the fringes without the object from the FTP result to align the reference plane. Then, imperfections outside the object area were removed by multiplying with a binary mask.

IV. RESULTS AND ERROR ANALYSIS

Two objects were analyzed to verify the functionality of the code and compare the reconstructed height to the real height. The first was Figure 8, which is compared with its result in Figure 9.



FIG. 8. Plaster figurine (“Monita”).

Next, a comparison is shown between the obtained results and the post-processed result in Figure 9.

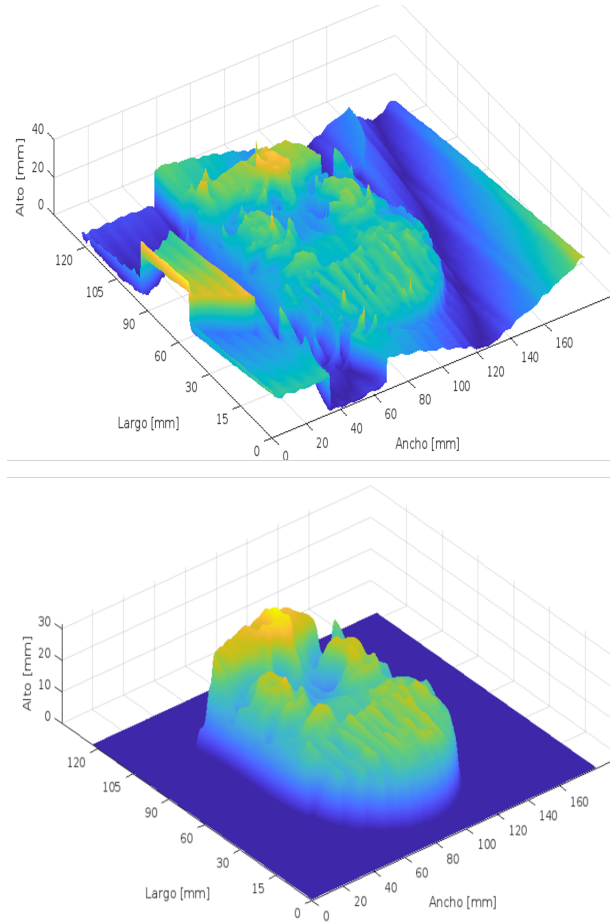


FIG. 9. Original FTP and post-processed FTP.

From these data, the errors were obtained:

Object region	True height (mm)	FTP height (mm)	Error %
Mouth	24	26	8.3%
Hair	24	22	8.3%
Side	19	17	8.3%
Eye	22	21	4.5%
Eyebrow	23	24	4.5%

TABLE I. Comparison between true height and reconstructed height, including the percentage error.

The next figure is a Styrofoam sphere (Figure 10) and it was compared with its result in Figure 11.

In this case, a single measurement was made and the percentage error was 8.3%. Therefore, the final error estimated from both objects was 6.8%, which is considered an acceptable and meaningful error for medium-resolution dimensional analysis.



FIG. 10. Experimental configuration.

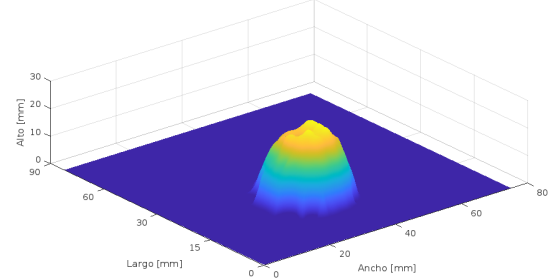


FIG. 11. Experimental configuration.

V. CONCLUSIONS

The application of appropriate methodologies enabled the 3D reconstruction of objects using fringe projection. During the experimental process, several projection methods were explored, including the use of an interferometer. However, our main challenge was generating images suitable for Fourier analysis, since one limitation of the method is the high definition required in the images, as well as the need for clear, low-noise fringe patterns. Despite these challenges, the Fourier method stands out for its speed and its ability to produce valuable results even with images that are not perfect. A suggested application for this method is its implementation in retail packaging lines, as in the case of Amazon. There, algorithms such as ELAS are used to estimate dimensions and select appropriate box sizes for packing objects; however, these algorithms are slower and require more computational resources than FTP. Therefore, FTP could represent a significant improvement in this context.

This project provided invaluable experience in scientific research and enabled effective application of knowledge acquired in the optics laboratory. For future work, it is suggested to improve the quality of the images used in FTP and explore the use of principal component analysis (PCA)[9] in spectral filtering to achieve even higher resolution in 3D reconstructions.

-
- [1] M. Takeda and K. Mutoh, Fourier transform profilometry for the automatic measurement of 3-d object shapes, *Appl. Opt.* **22**, 3977 (1983).
- [2] J. C. Pedraza-Ortega, E. Gorrostieta-Hurtado, J. M. Ramos-Arreguin, S. L. Canchola-Magdaleno, M. A. Aceves-Fernandez, M. Delgado-Rosas, and R. A. Rico-Hernandez, A profilometric approach for 3d reconstruction using fourier and wavelet transforms, in *MICAI 2009: Advances in Artificial Intelligence*, edited by A. H. Aguirre, R. M. Borja, and C. A. R. Garcíá (Springer Berlin Heidelberg, Berlin, Heidelberg, 2009) pp. 313–323.
- [3] D. S. Mehta, K. Saxena, S. K. Dubey, and C. Shakher, Coherence characteristics of light-emitting diodes, *Journal of Luminescence* **130**, 96 (2010).
- [4] Samsung Electronics Co., Ltd., HighPower LED C-SeriesGen3 3WWhite SPHWH1A1N3A0 - Product Family Data Sheet, Product Family Data Sheet (2022), Product Family Data Sheet Rev.1.8, 2022.05.26.
- [5] L. Chen and C. Quan, Fringe projection profilometry with nonparallel illumination: a least-squares approach, *Optics Letters* **30**, 2101 (2005).
- [6] S. Esquivel-Hernandez, R. Juarez-Salazar, and V. H. Diaz-Ramirez, First-order spectrum filtering in Fourier transform profilometry: a method comparison, in *Optics and Photonics for Information Processing XVII*, Vol. 12673 (SPIE Optical Engineering + Applications, 2023) p. 1267308, event: SPIE Optical Engineering + Applications, 2023, San Diego, California, United States.
- [7] L.-C. Chen, H.-W. Ho, and X.-L. Nguyen, Fourier transform profilometry (ftp) using an innovative band-pass filter for accurate 3-d surface reconstruction, *Optics and Lasers in Engineering* **48**, 182 (2010), fringe Projection Techniques.
- [8] Z. Zhao, Robust 2d phase unwrapping algorithm, MATLAB Central File Exchange (2024), retrieved May 7, 2024.
- [9] S. Feng, Q. Chen, C. Zuo, J. Sun, T. Tao, and Y. Hu, A carrier removal technique for fourier transform profilometry based on principal component analysis, *Optics and Lasers in Engineering* **74**, 80 (2015).

Appendices